

Electron Acceleration in a plasma produced from a dense gas jet irradiated by an intense laser pulse

M. Adachi¹⁾, E. Miura²⁾, S. Kato²⁾, N. Saito²⁾, K. Koyama²⁾, Y. Kawada³⁾, T. Nakamura⁴⁾
and M. Tanimoto⁵⁾

¹⁾*Graduate school of Advanced Science of Matter, Hiroshima University,
Higashi-Hiroshima, Hiroshima 739-8530, Japan*

²⁾*National Institute of Advanced Industrial and Science Technology (AIST),
Tsukuba, Ibaraki 305-8568, Japan*

³⁾*University of Tsukuba, Tsukuba, Ibaraki 305-8571, Japan*

⁴⁾*National Institute of Radiological Sciences (NIRS), Chiba, Chiba 263-8555, Japan*

⁵⁾*Meisei University, Hino, Tokyo 191-8506, Japan*

Introduction

Research on electron acceleration in a plasma produced by an intense laser pulse has been performed [1]. We performed experiments using a plasma (the electron density, $n_e \sim 10^{20} \text{ cm}^{-3}$) produced by an intense (2TW) and short laser pulse (the laser pulse duration, $\tau_L = 50 \text{ fs}$). In our experimental condition ($\omega_p \tau_L \sim 28$), proposed acceleration mechanisms were the self-modulated laser wakefield acceleration (SMLWFA) [2] and the direct laser acceleration (DLA) [3,4]. Here, ω_p and τ_L are the plasma frequency and the laser pulse duration, respectively. There have been few reports on electron acceleration experiments in a plasma ($n_e \geq 10^{20} \text{ cm}^{-3}$) produced by a laser pulse shorter than 50 fs [5] and have not been clarified the energetic electron acceleration mechanism.

Experiment

The experiment was performed with a 2-TW Ti:sapphire laser system, which delivered an energy of 100 mJ in duration of 50 fs. The center wavelength was 800 nm. The laser beam was focused on a gas jet by an off-axis parabolic mirror (165mm focal length, f/3.3). The focal position was $\sim 1 \text{ mm}$ away from the center of the nozzle and adjusted to the position where the largest number of energetic electrons were observed. The average intensity in a focal spot diameter of $5 \mu \text{ m}$ in a vacuum was $5 \times 10^{18} \text{ W/cm}^2$, which corresponds to the normalized vector potential a_0 of 1.5. A nitrogen (N_2) gas jet

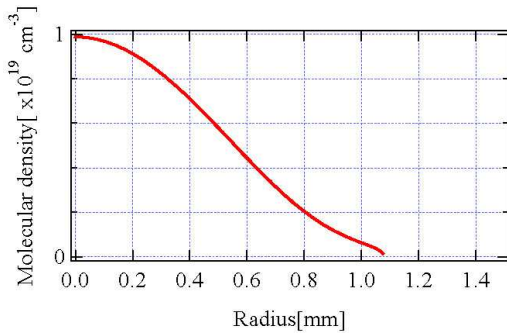


Fig. 1 The molecular density profile of the N₂ gas jet.

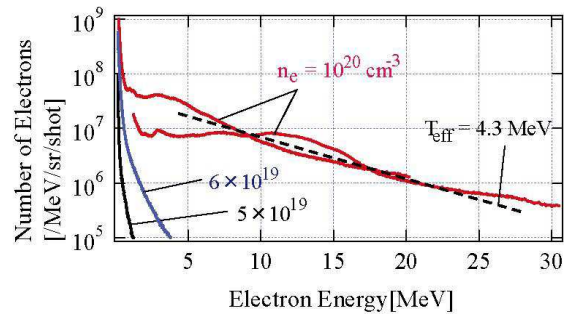


Fig. 2 Electron density dependence of electron energy spectra.

was ejected from a supersonic nozzle with an exit diameter of 1.5 mm. Figure 1 shows the N₂ density profile at 1.5 mm from the exit measured by an interferometer when the reservoir pressure of the pulsed valve was 13 bar. Under our experimental conditions, the stable ionization to N⁵⁺ is expected. Then, the electron density was estimated to be $1 \times 10^{20} \text{ cm}^{-3}$ at the nozzle center. An energy spectrum of the electron beam was measured by an electron spectrometer (ESM) in the forward direction of the laser pulse propagation. A Fuji Imaging Plate (IP) was used as a detector. The measured electron energy range was from 0.2 to 30 MeV. In order to clarify the electron acceleration mechanism, we also observed a spectrum of the forward scattered light as well as the side scattering light image.

Figure 2 shows the electron energy spectra for various electron densities from 5×10^{19} to $1 \times 10^{20} \text{ cm}^{-3}$ by changing the reservoir pressure of the pulsed valve. At an electron density of 10^{20} cm^{-3} , the spectrum had the Boltzmann-like distribution with an electron effective temperature of 4.3 MeV. The maximum electron energy was 30 MeV and the total number of electrons above 1 MeV was 10 pC/shot. Figure 3 shows a typical forward scattering light spectrum at the electron density of $1 \times 10^{20} \text{ cm}^{-3}$. The first Stokes satellite peak of forward Raman scattering was observed at around 1000 nm. From the wavelength of the satellite, an electron density of the region where the plasma waves were excited is estimated to be $\sim 10^{20} \text{ cm}^{-3}$ considering relativistic effect of $a_0 = 1.5$. When the Stokes satellite was observed, the strong side scattered image with the length of over 400 μm shown in Fig. 4 was simultaneously observed. This region exists from $\sim 400 \mu\text{m}$ before the nozzle center to the center. These two results suggest that the plasma waves were excited in the region with the electron density of $\sim 10^{20} \text{ cm}^{-3}$

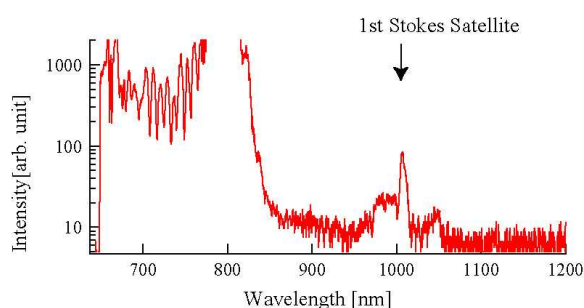


Fig. 3 A forward scattered light spectrum

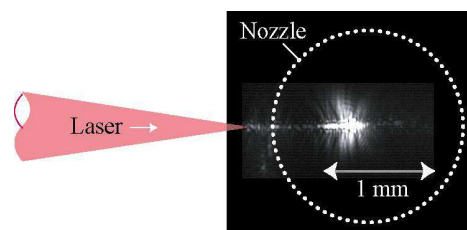


Fig. 4 A side scattered light image through interference filter of 800 nm. A dotted circle shows the nozzle exit.

in the length of over $400 \mu\text{m}$. When the electron density decreased from $1 \times 10^{20} \text{ cm}^{-3}$ to 5×10^{19} , the maximum electron energy and the total charge of the energetic electrons ($> 1 \text{ MeV}$) decreased.

Discussion

Here, we discuss the electron acceleration mechanism. It is clear that the SMLWFA contributed to the electron acceleration, because the excitation of plasma waves at $n_e = 1 \times 10^{20} \text{ cm}^{-3}$ was confirmed from the spectrum shown in Fig. 3. The strong side scattering shown in Fig. 4 correlated with the appearance of the Stokes satellite peak and was observed, without any significant changes in the length and position even at the lower density plasma ($5 \sim 6 \times 10^{19} \text{ cm}^{-3}$). Then, we consider that the electron plasma waves were excited at the lower density. If the plasma waves were excited in the strong side scattering region, the length of the region (over $400 \mu\text{m}$) is sufficient long to cause the wave breaking. In SMLWFA, the maximum electron energy is approximately proportional to $1/n_e$ assuming $\gamma_p \gg 1$. Here, γ_p is the ratio of the laser frequency to the plasma frequency. However, when the electron density decreased from 1×10^{20} to $6 \times 10^{19} \text{ cm}^{-3}$, the maximum electron energy decreased. This energy reduction might be caused by the disappearance of the wave breaking in SMLWFA. The length needed for the wake field to reach the wave breaking limit field becomes longer, as the electron density decreases. Therefore, at lower electron density, the wave breaking might not occur and the maximum energy and the total charge of the energetic electrons ($> 1 \text{ MeV}$) decreased. On the other hand, the observed maximum electron energy (30 MeV) was higher than the estimated value in SMLWFA (20 MeV) for the linear wave breaking

limit field. Then, we consider that the electrons were accelerated by both SMLWFA and DLA in our experimental condition. If the wave breaking did not occur at electron density of under $6 \times 10^{19} \text{ cm}^{-3}$, the electron acceleration by DLA was the dominant mechanism at that density region. Then, we consider that the energy reduction occurred from the electron density of 6×10^{19} to $5 \times 10^{19} \text{ cm}^{-3}$ was caused by the suppression of the relativistic self-focusing (RSF) effect. The threshold power of RSF increases, as the electron density decreases; then, the laser power focused in the channel by RSF decreases and the maximum electron energy decreases in DLA.

We, therefore, considered that both SMLWFA and DLA contributed to the electron acceleration in our experimental conditions. Using particle in cell simulation, in Ref. 6, it has been shown that both SMLWFA and DLA contribute to electron acceleration under the condition close to our experimental condition ($n_e = 1 \times 10^{20} \text{ cm}^{-3}$, $a_0 \sim 1.0$ and $\omega_p \tau_L \sim 17$).

Summary

The maximum electron energy observed was 30 MeV and the total charge of the electrons ($> 1 \text{ MeV}$) was 10 pC. The Stokes satellite peak was observed at the electron density of $1 \times 10^{20} \text{ cm}^{-3}$. We consider that both SMLWFA and DLA contributed to the energetic electron acceleration in our experimental conditions ($a_0 = 1.5$ and $\omega_p \tau_L = 28$).

This work was supported by the Budget for Nuclear Research of the MEXT and the Advanced Accelerator Project of the MEXT.

References

- [1] D. Umstadter, et al., J. Phys. D., **36** R151 (2003).
- [2] J. Krall, et al., Phys. Rev. E, **48** 2157 (1993).
- [3] A. Pukhov, et al., Phys. Plasmas, **6** 2847 (1999).
- [4] C. Gahn, et al., Phys. Rev. Lett. **83**, 4772 (1999).
- [5] V. Malka, et al., Phys. of Plasmas, **8** 2605 (2001).
- [6] A. Pukhov, et al., Appl. Phys. B, **74** 355 (2002).